ACS Medicinal Chemistry Letters

Letter

pubs.acs.org/acsmedchemlett

Discovery of Brain-Penetrant, Irreversible Kynurenine Aminotransferase II Inhibitors for Schizophrenia

Amy B. Dounay,* Marie Anderson, Bruce M. Bechle, Brian M. Campbell, Michelle M. Claffey, Artem Evdokimov, Edelweiss Evrard, Kari R. Fonseca, Xinmin Gan, Somraj Ghosh, Matthew M. Hayward, Weldon Horner, Ji-Young Kim, Laura A. McAllister, Jayvardhan Pandit, Vanessa Paradis, Vinod D. Parikh, Matthew R. Reese, SuoBao Rong, Michelle A. Salafia, Katherine Schuyten, Christine A. Strick, Jamison B. Tuttle, James Valentine, Hong Wang, Laura E. Zawadzke, and Patrick R. Verhoest

Pfizer Worldwide Research and Development, Neuroscience Chemistry, Eastern Point Road, Groton, Connecticut 06340, United States

Supporting Information

ABSTRACT: Kynurenine aminotransferase (KAT) II has been identified as a potential new target for the treatment of cognitive impairment associated with schizophrenia and other psychiatric disorders. Following a high-throughput screen, cyclic hydroxamic acid PF-04859989 was identified as a potent and selective inhibitor of human and rat KAT II. An X-ray crystal structure and ^{13}C NMR studies of PF-04859989 bound to KAT II have demonstrated that this compound forms a covalent adduct with the enzyme cofactor, pyridoxal phosphate (PLP), in the active site. In vivo pharmacokinetic and efficacy studies in rat show that PF-04859989 is a brain-penetrant, irreversible inhibitor and is capable of reducing brain kynurenic acid by 50% at a dose of 10 mg/kg (sc). Preliminary structure−activity relationship investigations have been completed and have identified the positions on this scaffold best suited to modification for further optimization of this novel series of KAT II inhibitors.

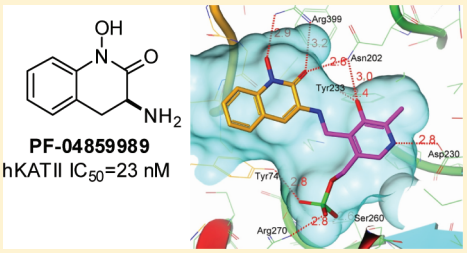

KEYWORDS: *KAT II, kynurenic acid, kynurenine aminotransferase, hydroxamic acid*

Kynurenic acid (KYNA, **3**) is a neuroactive metabolite produced in the kynurenine pathway of L-tryptophan degradation (Figure 1). Interest in the pharmacological

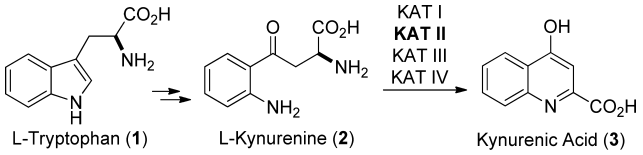

Figure 1. KYNA biosynthesis.

modulation of this pathway has been prompted by reports that KYNA is an inhibitor of α_7 nicotinic acetylcholine receptor function[1] and an antagonist at the glycine site of the *N*-methyl-D-aspartate (NMDA) receptor.[2] KYNA has also recently been identified as a potent agonist at the aryl hydrocarbon receptor (AHR).[3] A growing body of preclinical evidence suggests that KYNA is directly involved in the pathophysiology of schizophrenia,[4] among other psychiatric and neurological disorders.[5,6] Elevated KYNA levels have been observed in the cerebrospinal fluid[7,8] and postmortem prefrontal cortex[9] of schizophrenia patients. Studies have also shown an elevation of KYNA in the cerebrospinal fluid of patients with bipolar disorder.[10] Thus, the reduction of KYNA levels in the brain via modulation of the kynurenine pathway may provide a novel treatment for schizophrenia and other diseases of the central nervous system (CNS).

The synthesis of KYNA in the brain is catalyzed primarily by astrocytic kynurenine aminotransferases KAT I and KAT II.[11] KAT II is currently viewed as the major determinant of KYNA biosynthesis in rat and human brain. An X-ray structure of the homodimeric human KAT II complex bound to its endogenous cofactor, pyridoxal-5′-phosphate (PLP), has been reported, and unique structural features of this enzyme suggest the possibility of structure-based design of isozyme-specific inhibitors.[12] The recent X-ray structure of human KAT II bound to the selective inhibitor BFF-122 further confirms that structure-based design strategies may be useful for the design and optimization of selective KAT II inhibitors.[13]

Several recent studies have employed the selective tool compounds (*S*)-ESBA (**4**) and BFF-122 (**5**, Figure 2) via central administration for study of KAT II inhibition in preclinical models.[14−18] However, identification of brain-penetrant KAT II inhibitors with druglike properties remains a challenge. Additionally, recent reports have established that sequence variants in human and rat KAT II cause significant cross-species enzyme potency shifts for inhibitor **4**.[19,20] Our primary objective was to

Received: August 18, 2011
Accepted: January 16, 2012
Published: January 25, 2012

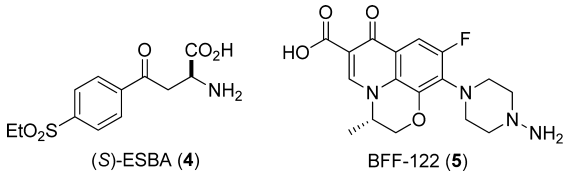

Figure 2. Selective KAT II inhibitors.

identify a selective, brain-penetrant tool compound for further exploration of KAT II inhibition in preclinical models of schizophrenia and cognition. Identification of a series of KAT II inhibitors with submicromolar binding affinity at both the rat and the human isoforms of KAT II would facilitate preclinical studies and clinical candidate identification. To enable rapid series optimization toward a clinical therapeutic agent, our criteria for novel lead compounds included high ligand efficiency[21] (LE > 0.35) and excellent drug-like physicochemical properties (MW, log *P*, polar surface area).[22−24]

In an effort to identify novel KAT II inhibitors, a high-throughput screen of the Pfizer compound file was conducted. Aminodihydroquinolone **6** (Figure 3) initially emerged as an

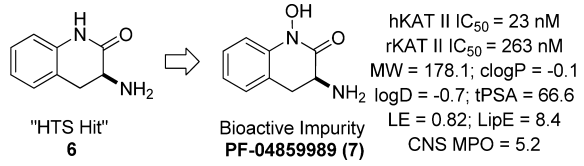

Figure 3. Properties of HTS hit PF-04859989 (7).

interesting hit, but follow-up testing of an authentic sample of **6** demonstrated that this compound had no significant inhibitory activity toward hKAT II. Chromatographic separation, characterization, resynthesis, and screening of minor impurities from the original HTS sample batch led to the identification of (3*S*)-3-amino-1-hydroxy-3,4-dihydroquinolin-2(1*H*)-one (PF-04859989, **7**) as the active constituent (hKAT II IC_{50} = 23 nM) from the HTS sample. Because of its high potency and low molecular weight (178 Da), compound **7** is an attractive hit from the standpoint of ligand efficiency (LE = 0.82). Furthermore, other physicochemical properties of **7** (clog *P* = −0.1, tPSA[25] = 66.6, and CNS MPO score[26] = 5.2), combined with its clean profile in the standard CEREP panel,[27] position **7** in excellent chemical space for a lead compound targeting the CNS.[28] Compound **7** is also selective for KAT II over human KAT I, KAT III, and KAT IV (IC_{50} values of 22, 11, and >50 μM, respectively).[29] Finally, the modest potency shift (~10×) between human and rat KAT II (rKAT II IC_{50} = 263 nM) suggests that compounds of this type could serve as useful tools in preclinical rodent models.

An X-ray crystal structure (3.2 Å) of **7** bound to human KAT II reveals several key interactions that account for the remarkable potency and selectivity of this inhibitor (Figure 4).[30] First, the

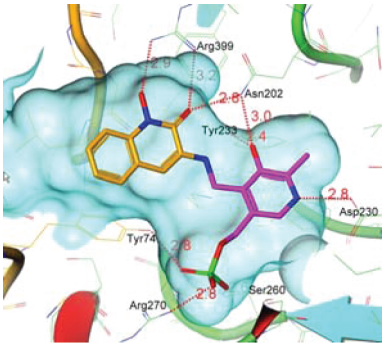

Figure 4. X-ray structure of KAT II-PLP adduct with **7** (carbon scaffold from **7** in orange and PLP in magenta). A cutaway section of the molecular surface forming the catalytic site of KAT II is shown in pale blue. The substrate-binding pocket is formed by residues from both subunits of the KAT II dimer, one colored in green and the other in orange. Hydrogen bond interactions between the ligand and the protein are indicated as dotted lines, with distances indicated in Å.

X-ray structure indicates that **7** is covalently attached to PLP in the active site of KAT II, via a linkage between the primary amine of **7** and the aldehyde functionality of PLP. At the resolution of this structure, the two most likely adduct structures, a Schiff base **I** and enamine **II** (Scheme 1), are indistinguishable, but additional NMR studies have confirmed the enamine structure (vide infra). A series of dialysis and kinetic studies were carried out to further characterize this adduct, confirming that it is formed irreversibly.[31] This covalent adduct bears a number of similarities to the recently reported KAT II-bound adduct formed between PLP and inhibitor BFF-122 (**5**).[13] As in the case of **5**, the formation of a covalent adduct between **7** and PLP is crucial to the observed potency of this inhibitor. The PLP portion of the adduct, although not covalently linked to KAT II, maintains numerous H-bond donor−acceptor interactions with the enzyme, as detailed in the previously reported human KAT II-PLP structure.[12] For example, the nitrogen atom of the pyridine ring of PLP interacts with the highly conserved Asp-230 residue, whose side chain is held in place by a hydrogen bond to the OH group of Tyr-195. Likewise, the PLP O3′ atom forms hydrogen bonds with Tyr-233 and Asn-202. The PLP phosphate group participates in a network of hydrogen-bonding interactions, including contacts with Ser-262, Arg-270, Ser-117, Gln-118, and Ser-260 of one subunit and Tyr-74 of the other

Scheme 1. Postulated Imine−Enamine Isomerization of the PF-04859989-PLP Adduct

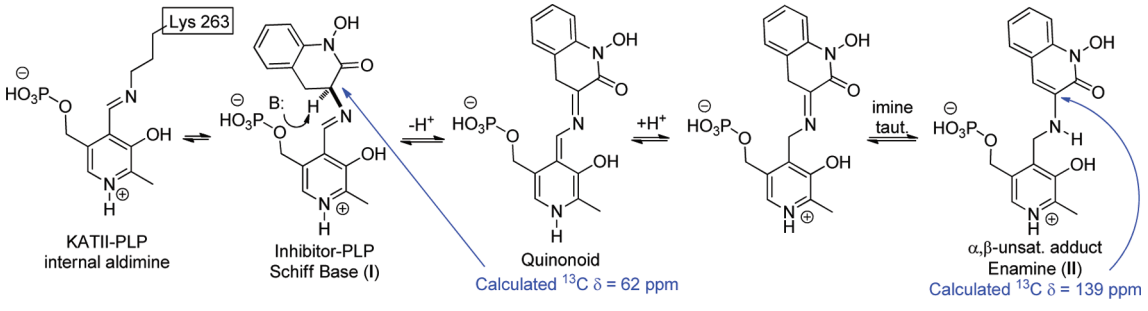

dx.doi.org/10.1021/ml200204m | ACS Med. Chem. Lett. 2012, 3, 187−192

subunit. The other two elements of the functional triad of the 3-aminohydroxamic acid moiety of **7** also contribute key binding interactions: the carbonyl oxygen of **7** serves as an H-bond acceptor in an interaction with the side chain of Asn-202, and the other oxygen atom in the hydroxamic acid functionality of **7** accepts a hydrogen bond from Arg-399. The fused phenyl group of **7** contributes to van der Waals interactions with the hydrophobic pocket formed by Leu-40, Tyr-74, and Leu-293.

To definitively characterize the KAT II-PLP adduct observed in the X-ray structure, a series of protein NMR experiments were designed to distinguish between the Schiff base **I** and the enamine adduct **II**, the two most likely covalent inhibitor structures (Scheme 1). The detailed studies by Silverman and co-workers on cycloserine inhibition of γ-amino butyric acid aminotransferase (GABA-AT), another PLP-dependent enzyme, demonstrated that initial Schiff base formation between cycloserine and PLP in the enzyme active site is followed by a series of proton transfer events, which ultimately lead to aromatization of the cycloserine adduct.[32,33] By analogy, we anticipated that the initially formed Schiff base adduct between **7** and PLP in the KAT II active site may undergo a series of proton transfers, leading to the formation of a more stable isomeric α,β-unsaturated (aromatized) product. The incorporation of a ^{13}C label into our inhibitor, affording the isotopic analogue **7a**, provided a dramatic signal enhancement of the labeled carbon atom in the ^{13}C NMR spectra. Predicted ^{13}C chemical shifts for the labeled carbon in **7a** were significantly different for the Schiff base **I** (62 ppm) as compared to the α,β-unsaturated adduct **II** (139 ppm).[34] NMR experiments examining **7a** in a buffer solution (not shown) and in a solution containing KAT II without PLP (Figure S1A in the Supporting Information)[35] revealed a distinctive ^{13}C signal at 50 ppm. Upon addition of PLP to the KAT II inhibitor solution (Figure S1B in the Supporting Information), the signal at 50 ppm disappeared and a new signal appeared at 137 ppm, consistent with the formation of the α,β-unsaturated adduct **II**.[36]

Guided by the X-ray structure of **7** bound to KAT II, we sought to build an understanding of the structural requirements for potent and selective inhibition of KAT II within this series of irreversible inhibitors. Although irreversible inhibition was not one of our lead criteria at the outset of the program, maintaining this attribute of **7** was a high priority through our optimization efforts. The potential advantages of irreversible inhibitors include low dose requirements and reduced off-target toxicity.[37,38] Furthermore, this irreversible inhibitor does not covalently bind to the protein, which should significantly reduce the potential for an immune response. To fully explore the structure–activity relationship (SAR) around the PF-04859989 scaffold, several synthetic approaches were developed (see Scheme 2); detailed descriptions of these methods have recently been disclosed.[39,40] In general, the synthesis of **7** and its analogues requires access to α-amino acids or α-amino esters, which undergo reductive cyclization to afford 3-amino-1-hydroxy-3,4-dihydroquinolin-2(1*H*)-ones. In the case of **7** itself, direct catalytic reductive cyclization using Pt/C and H_2 (method A) provided clean conversion to the desired product without competitive over-reduction to the corresponding lactam. However, for substituted analogues, alternate cyclization conditions were generally required to minimize over-reduction of the nitro functionality. Cyclization with $SnCl_2$ in the presence of NaOAc (method C) generally provided 5-, 6-, or 7-substituted 3-amino-1-hydroxy-3,4-dihydroquinolin-2(1*H*)-ones in good yield. However, efficient conversion to 8-substituted

Scheme 2. Synthesis of Hydroxamic Acids 7–27

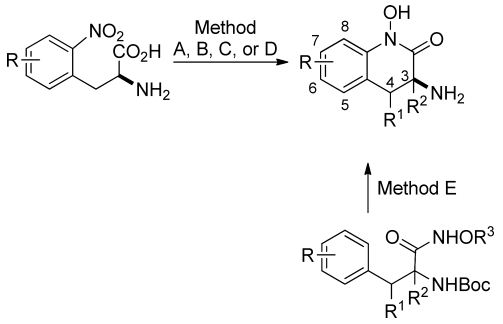

Reagents and conditions: Method A: (i) Pt/C, pyridine, H_2. (ii) HCl/MeOH. Method B: Pt/C, MeOH, HCl, H_2. Method C: (i) $SnCl_2$, NaOAc, THF. (ii) Boc_2O, Et_3N. (iii) HCl. Method D: (i) Boc_2O, Et_3N. (ii) CF_3CH_2OTf. (iii) Pt/C, pyridine, H_2. (iv) HCl. Method E: (i) phenyliodine(III) bis(trifluoroacetate) (PIFA), CH_2Cl_2. (ii) BF_3 diethyl etherate, THF.

analogues (e.g., **13–16**) required activation of the carboxylic acid to the trifluoroethyl ester prior to cyclization (method D). An oxidative cyclization approach using phenyliodine(III) bis(trifluoroacetate) (PIFA, method E) also provided ready access to select analogues in the series (e.g., **9** and **11**).

Our preliminary SAR studies on the 3-amino-1-hydroxy-3,4-dihydroquinolin-2(1*H*)-one template explored the role of stereochemistry of the 3-amino group and the effects of substituents at the 1-, 3-, and 4-positions. Comparison of **7** [(3*S*)-amino-1-hydroxy-3,4-dihydroquinolin-2(1*H*)-one] with its enantiomer **8** demonstrated that the (*S*)-enantiomer is ~10-fold more potent, with similar shifts against both human and rat enzymes. This enantiopreference in inhibition of KAT II correlates with the stereochemistry of the enzyme's substrate, L-kynurenine (**2**) [(*S*)-2-amino-4-(2-aminophenyl)-4-oxobutanoic acid]. Methyl hydroxamate **9** displayed a complete loss of activity at KAT II, indicating that a free hydroxamic acid group is crucial in this series. Likewise, introduction of a methyl group at the C3-position (compound **10**) resulted in complete loss of activity. This finding may be explained by the possibility of unfavorable steric interactions between this methyl group and Leu 293 and/or Tyr 142 in this region of the binding pocket. Furthermore, this SAR observation is consistent with our NMR studies of **7a**, which demonstrated that a hydrogen substituent at C3 is mechanistically required for potent, irreversible inhibition. The addition of a methyl group at the C4 position (compound **11**) also led to significant loss of activity. In brief, the preliminary SAR work around positions 1–4 of PF-04859989 demonstrate that the (*S*)-configuration is preferred and that even minor modifications within this domain lead to dramatic loss of KAT II potency. These SAR findings are consistent with our X-ray structure and mechanistic studies, which suggest that each moiety in this aminohydroxamic acid functional group triad forms a key interaction with KAT II. Furthermore, introduction of any adjacent substituents that interfere with the formation of the inhibitor–PLP enamine adduct in the KAT II active site also leads to significant potency loss.

Next, the effects of introducing substituents at positions 5 through 8 on the 3-amino-1-hydroxy-3,4-dihydroquinolin-2(1*H*)-one template were explored (Table 2). The relative potency of analogues was initially assessed by evaluating IC_{50} values from our human and rat KAT II enzyme assays. These studies demonstrated that only small R^1 substituents (R^1 = F, compound **12**) are tolerated by human KAT II. Significant loss of potency is observed with even slightly larger substituents at

dx.doi.org/10.1021/ml200204m | ACS Med. Chem. Lett. 2012, 3, 187–192

Table 1. Human and Rat KAT II Potency for Analogues of 7

Cmpd	Structure	Synthetic Method	hKAT II IC_{50}[a] (nM)	rKAT II IC_{50}[a] (nM)
6	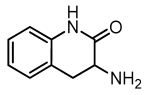	--	>10,000	--
7	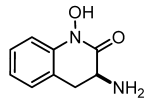	A	23	263
8	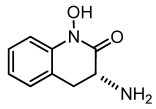	A	219	1170
9	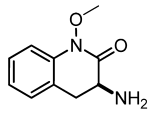	E	>10,000[b]	>10,000
10	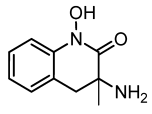	B	>10,000	>10,000[c]
11	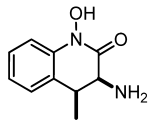	E	3280[b]	>1330[b]

[a]Values represent the geometric mean of at least three independent determinations. [b]n = 1. [c]n = 2.

this position (compounds **13**–**16**). Interestingly, the rat KAT II enzyme is even more sensitive than the human enzyme to substitution at this position, with complete loss of activity observed for compounds **13**–**16**. The evaluation of R^4 substituents likewise demonstrated that only small groups (R^4 = F, compound **23**) are tolerated at this position. All compounds with larger R^4 substituents (compounds **24**–**27**) are significantly less potent than **7**. This potency loss is likely due to unfavorable steric interactions between the R^4 substituents and the Tyr74 and Leu293 in hKAT II. These larger R^4 substituents, like the R^1 substituents, also bring about complete loss of rat KAT II potency. Evaluation of R^2 and R^3 substituents revealed that both the human and the rat KAT II enzymes are less sensitive to small changes at these positions. The addition of small R^2 (Cl, Me, OMe) or R^3 (Cl, Me, CF_3) groups[41] to **7** does not appear to dramatically affect the human or rat KAT II potency: human and rat KAT II IC_{50} values for analogues **17**–**22** are within 2-fold of the respective values for **7**. Our assessment of steric and electronic effects of R^1–R^4 in this series (e.g., MeO vs Cl, CF_3) suggests that electronic effects do not drive the SAR. These preliminary SAR data suggest that the R^2 and R^3 positions hold the most promise for further SAR work to optimize properties and potency for this series.

To ensure a rigorous evaluation of SAR within this series of irreversible inhibitors, potency was also assessed in terms of the second order rate constant k_{inact}/K_i (Table 2). Unlike IC_{50} values, k_{inact}/K_i values are independent of substrate concentration and preincubation time and are considered the best measure of potency for irreversible inhibitors.[42] In the case of **7** and its analogues **12**–**27**, the IC_{50} potency trends are paralleled by the k_{inact}/K_i values. The k_{inact}/K_i values indicate a subtle differentiation of compounds **17**–**19** from **7**, suggesting that small R^2 substituents may provide a boost in potency. This trend was not observed in the IC_{50} SAR, perhaps due in part to the relatively high enzyme concentration (30 nM) employed in that assay format.

Table 2. Human and Rat KAT II Potency for Analogues of 7

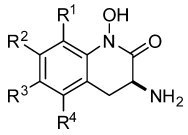

					IC_{50}[a] (nM)		k_{inact}/K_i[b] (M^{-1} s^{-1})	
compd	R^1	R^2	R^3	R^4	hKAT II	rKAT II	hKAT II	rKAT II
7	H	H	H	H	23	263	18 500	573
12	F	H	H	H	40	631	5310	57
13	OMe	H	H	H	572	>10 000	21.3	
14	Cl	H	H	H	252	>10 000	42.0	
15	Me	H	H	H	1050[c]	>10 000[c]		
16	CF_3	H	H	H	174	>6810	541	
17	H	Cl	H	H	29	118	28 300	1170
18	H	Me	H	H	37	368	33 400	590
19	H	OMe	H	H	22	137	31 700	1840
20	H	H	Cl	H	36	258	19 000	465
21	H	H	Me	H	30	402	11 900	167
22	H	H	CF_3	H	29	488	15 300	102
23	H	H	H	F	45	2060	6680	
24	H	H	H	Cl	349	>7970	9.5	
25	H	H	H	Me	319	>10 000		
26	H	H	H	OMe	179	>4920	1940	
27	H	H	H	CF_3	>10 000	>10 000		

[a]Values represent the geometric mean of at least three experiments. [b]Values represent the arithmetic mean of at least three experiments. Additional statistical details are provided in the Supporting Information. [c]n = 2.

dx.doi.org/10.1021/ml200204m | ACS Med. Chem. Lett. 2012, 3, 187–192

Compound 7 was selected as a protypical tool compound for evaluation of the in vivo characteristics of this series of KAT II inhibitors. In vivo pharmacokinetic experiments were carried out to evaluate the utility of 7 as a systemically dosed tool compound. Compound 7 displayed excellent CNS exposure in rat after subcutaneous administration (Table 3). This compound displays relatively high free fraction in rat brain and plasma protein binding assays and is brain-penetrant, with a free plasma:free brain:CSF exposure ratio of 2.7:1:1.1.

Table 3. Rat Fractions Unbound and Plasma, Brain, and CSF Exposure for 7

fraction unbound		concn[a] (nM)		
brain	plasma	free plasma	free brain	CSF
39.3	89.3	10200 ± 403	3760 ± 776	4060 ± 969

[a]Drug concentrations measured at 0.25 h time point, 10 mg/kg sc dose.

In vivo efficacy of 7 was confirmed by measuring KYNA in dialysates from prefrontal cortex in freely moving rats. At the drug exposures described in Table 3 (dose, 10 mg/kg sc), KYNA concentrations decreased to approximately 50% of basal values (Figure 5).[43] This decrease was achieved approximately 1 h after dosing, and KYNA concentrations returned to baseline levels approximately 20 h postdose. This prolonged duration of action is attributable to the irreversible inhibition of KAT II by 7.

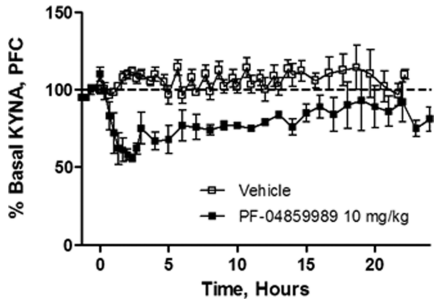

Figure 5. PF-04859989 (10 mg/kg, sc) was dosed at time = 0. The KYNA concentration was monitored over time in rat prefrontal cortex using microdialysis, as described in the Supporting Information. Data, expressed as percent of basal KYNA of each individual, are plotted as means ± SEMs, n = 11−14 animals per group.

In conclusion, 7 is a potent, brain-penetrant KAT II inhibitor that exhibits all of the necessary attributes to serve as a pharmacological tool for building confidence in the biological rationale of this target. As irreversible inhibitors of KAT II, compounds in this series may have unique advantages as potential clinical candidates. Preliminary SAR investigations have identified that the R^2 and R^3 positions on this scaffold are ideal for additional modifications to optimize properties and potency for this series. Future publications will detail the further elaboration of this series and advancement of our understanding of structural−functional relationships for this unique series of irreversible inhibitors of KAT II.

■ ASSOCIATED CONTENT

Supporting Information

Experimental procedures for the synthesis of 7−27, assay protocols, and CEREP screening data for 7. This material is available free of charge via the Internet at http://pubs.acs.org.

■ AUTHOR INFORMATION

Corresponding Author

*Tel: (860)-686-9208. E-mail: amy.dounay@pfizer.com.

Notes

The authors declare no competing financial interest.

■ ACKNOWLEDGMENTS

We gratefully acknowledge Larry James for KAT III screening, Kevin Parris for help with the final x-ray refinement, and Katherine Brighty for careful editing of this manuscript.

■ REFERENCES

(1) Hilmas, C.; Pereira, E. F.; Alkondon, M.; Rassoulpour, A.; Schwarcz, R.; Albuquerque, E. X. The Brain Metabolite Kynurenic Acid Inhibits α7 Nicotinic Receptor Activity and Increases Non-α7 Nicotinic Receptor Expression: Physiopathological Implications. *J. Neurosci.* **2001**, *21*, 7463−7473.

(2) Kessler, M.; Terramani, T.; Lynch, G.; Baudry, M. A Glycine Site Associated with N-Methyl-D-Aspartic Acid Receptors: Characterization and Identification of a New Class of Antagonists. *J. Neurochem.* **1989**, *52*, 1319−1328.

(3) Natale, B. C.; Murray, I. A.; Schroeder, J. C.; Flaveny, C. A.; Lahoti, T. S.; Laurenzana, E. M.; Omiecinski, C. J.; Perdew, G. H. Kynurenic Acid Is a Potent Endogenous Aryl Hydrocarbon Receptor Ligand that Synergistically Induces Interleukin-6 in the Presence of Inflammatory Signaling. *Toxicol. Sci.* **2010**, *115*, 89−97.

(4) Erhardt, S.; Schwieler, L.; Nilsson, L.; Linderholm, K.; Engberg, G. The Kynurenic Acid Hypothesis of Schizophrenia. *Physiol. Behav.* **2007**, *92*, 203−209.

(5) Erhardt, S.; Olsson, S. K.; Engberg, G. Pharmacological Manipulation of Kynurenic Acid: Potential in the Treatment of Psychiatric Disorders. *CNS Drugs* **2009**, *23*, 91−101.

(6) Potter, M. C.; Elmer, G. I.; Bergeron, R.; Albuquerque, E.; Guidetti, P.; Wu, H.-Q.; Schwarcz, R. Reduction of Endogenous Kynurenic Acid Formation Enhances Extracellular Glutamate, Hippocampal Plasticity, and Cognitive Behavior. *Neuropsychopharmacology* **2010**, *35*, 1734−1742.

(7) Erhardt, S.; Blennow, K.; Nordin, C.; Skogh, E.; Lindstrom, L. H.; Engberg, G. Kynurenic Acid Levels Are Elevated in the Cerebrospinal Fluid of Patients with Schizophrenia. *Neurosci. Lett.* **2001**, *313*, 96−98.

(8) Nilsson, L. K.; Linderholm, K. R.; Engberg, G.; Paulson, L.; Blennow, K.; Lindstrom, L. H.; Nordin, C.; Karanti, A.; Persson, P.; Erhardt, S. Elevated Levels of Kynurenic Acid in the Cerebrospinal Fluid of Male Patients with Schizophrenia. *Schizophr. Res.* **2005**, *80*, 315−322.

(9) Schwarcz, R.; Rassoulpour, A.; Wu, H.-Q.; Medoff, D.; Tamminga, C. A.; Roberts, R. C. Increased Cortical Kynurenate Content in Schizophrenia. *Biol. Psychiatry* **2001**, *50*, 521−530.

(10) Olsson, S. K.; Samuelsson, M.; Saetre, P.; Lindstrom, L.; Jonsson, E. G.; Nordin, C.; Engberg, G.; Erhardt, S.; Landen, M. Elevated Levels of Kynurenic Acid in the Cerebrospinal Fluid of Patients with Bipolar Disorder. *J. Psychiatry Neurosci.* **2010**, *35*, 195−199.

(11) For a recent review, see Han, Q.; Cai, T.; Tagle, D. A.; Li, J. Structure, Expression, and Function of Kynurenine Aminotransferases in Human and Rodent Brains. *Cell. Mol. Life Sci.* **2010**, *67*, 353−368.

(12) Rossi, F.; Garavaglia, S.; Montalbano, V.; Walsh, M. A.; Rizzi, M. Crystal Structure of Human Kynurenine Aminotransferase II, a Drug Target for the Treatment of Schizophrenia. *J. Biol. Chem.* **2008**, *283*, 3559−3566.

(13) Rossi, F.; Valentina, C.; Garavaglia, S.; Sathyasaikumar, K. V.; Schwarz, R.; Kojima, S.; Okuwaki, K.; Ono, S.; Kajii, Y.; Rizzi, M. Crystal Structure-Based Selective Targeting of the Pyridoxal 5′-Phosphate Dependent Enzyme Kynurenine Aminotransferase II for Cognitive Enhancement. *J. Med. Chem.* **2010**, *53*, 5684−5689.

(14) Pellicciari, R.; Rizzo, R. C.; Costantino, G.; Marinozzi, M.; Amori, L.; Guidetti, P.; Wu, H.-Q.; Schwarcz, R. Modulators of the

Kynurenine Pathway of Tryptophan Metabolism: Synthesis and Preliminary Biological Evaluation of (*S*)-4-(Ethylsulfonyl)-benzoylalanine, a Potent and Selective Kynurenine Aminotransferase II (KAT II) Inhibitor. *ChemMedChem* **2006**, *1*, 528−531.
(15) Amori, L.; Wu, H.-Q.; Marinozzi, M.; Pellicciari, R.; Guidetti, P.; Schwarcz, R. Specific Inhibition of Kynurenate Synthesis Enhances Extracellular Dopamine Levels in the Rodent Striatum. *Neuroscience* **2009**, *156*, 196−203.
(16) Amori, L.; Guidetti, P.; Pellicciari, R.; Kajii, Y.; Schwarcz, R. On the Relationship Between the Two Branches of the Kynurenine Pathway in the Rat Brain In Vivo. *J. Neurochem.* **2009**, *109*, 316−325.
(17) Wu, H.-Q.; Pereira, E. F. R.; Bruno, J. P.; Pellicciari, R.; Albuquerque, E. X.; Schwarcz, R. The Astrocyte-Derived α7 Nicotinic Receptor Antagonist Kynurenic Acid Controls Extracellular Glutamate Levels in the Prefrontal Cortex. *J. Mol. Neurosci.* **2010**, *40*, 204−210.
(18) Schwarcz, R.; Kajii, Y.; Ono, S. Preparation of amino-piperazinylquinolonecarboxylates as kynurenine-amino-transferase inhibitors. WO 2009064836.
(19) Pellicciari, R.; Venturoni, F.; Bellocchi, D.; Carotti, A.; Marinozzi, M.; Macchiarulo, A.; Amori, L.; Schwarcz, R. Sequence Variants in Kynurenine Aminotransferase II (KAT II) Orthologs Determine Different Potencies of the Inhibitor (*S*)-ESBA. *ChemMedChem* **2008**, *3*, 1199−1202.
(20) Casazza, V.; Rossi, F.; Rizzi, M. Biochemical and structural investigations on kynurenine aminotransferase II: an example of conformation-driven species-specific inhibition? *Curr. Top. Med. Chem.* **2011**, *11*, 148−157.
(21) Hopkins, A. L.; Groom, C. R.; Alex, A. Ligand Efficiency: A Useful Metric for Lead Selection. *Drug Discovery Today* **2004**, *9*, 430−431.
(22) Keserü, G. M.; Makara, G. M. The Influence of Lead Discovery Strategies on the Properties of Drug Candidates. *Nat. Rev. Drug Discovery* **2009**, *8*, 203−212.
(23) Price, D. A.; Blagg, J.; Jones, L.; Greene, N.; Wager, T. Physicochemical Drug Properties Associated with In Vivo Toxicological Outcomes: A Review. *Expert Opin. Drug Metab. Toxicol.* **2009**, *5*, 921−931.
(24) Edwards, M. P.; Price, D. A. Role of physicochemical properties and ligand lipophilicity efficiency in addressing drug safety risks. *Annu. Rep. Med. Chem.* **2010**, *45*, 381−391.
(25) Ertl, P.; Rohde, B.; Selzer, P. Fast calculation of molecular polar surface area as a sum of fragment-based contributions and its applications to the prediction of drug transport properties. *J. Med. Chem.* **2000**, *43*, 3714−3717.
(26) Wager, T. T.; Hou, X.; Verhoest, P. R.; Villalobos, A. Moving beyond Rules: The Development of a Central Nervous System Multiparameter Optimization (CNS MPO) Approach To Enable Alignment of Druglike Properties. *ACS Chem. Neurosci.* **2010**, *1*, 435−449.
(27) For details on the CEREP screening panel, see www.cerep.fr. The PF-04859989 screening data set is provided in the Supporting Information.
(28) Wager, T. T.; Chandrasekaran, R. Y.; Hou, X.; Troutman, M. D.; Verhoest, P. R.; Villalobos, A.; Will, Y. Defining Desirable Central Nervous System Drug Space through the Alignment of Molecular Properties, in Vitro ADME, and Safety Attributes. *ACS Chem. Neurosci.* **2010**, *1*, 420−434.
(29) Compound **7** has also been screened against the following list of PLP-dependent enzymes: human alanine aminotransferase (ALT) (IC_{50} = 96 nM), rat γ-aminobutyric acid (GABA) transaminase (2% inhibition at 10 μM), and human D-amino acid oxidase (DAAO) (IC_{50} > 50 μM).
(30) The coordinates have been deposited in the Protein Data Bank, with ID 3UE8.
(31) Anderson, M. Personal communication, Pfizer.
(32) Olson, G. T.; Fu, M.; Lau, S.; Rinehart, K. L.; Silverman, R. B. An Aromatization Mechanism of Inactivation of Gamma-Aminobutyric Acid Aminotransferase for the Antibiotic L-Cycloserine. *J. Am. Chem. Soc.* **1998**, *120*, 2256−2267.
(33) Cycloserine does not inhibit human or rat KAT II (IC_{50} > 10 000 nM in our assays).
(34) ACD Labs 9.0.
(35) Figure S1 is available in the Supporting Information.
(36) Control experiments have demonstrated that the nonenzymatic reaction between **7** and PLP does not proceed to an appreciable extent under these conditions.
(37) Johnson, D. S.; Weerapana, E.; Cravatt, B. F. Strategies for discovering and derisking covalent, irreversible enzyme inhibitors. *Future Med. Chem.* **2010**, *2*, 949−964.
(38) Singh, J.; Petter, R. C.; Baillie, T. A.; Whitty, A. The Resurgence of Covalent Drugs. *Nat. Rev. Drug Discovery* **2011**, *10*, 307−317.
(39) Claffey, M. M.; Dounay, A. B.; Gan, X.; Hayward, M. M.; Rong, S.; Tuttle, J. B.; Verhoest, P. R. Bicyclic and Tricyclic Compounds as KAT II Inhibitors. WO2010146488.
(40) McAllister, L. A.; Bechle, B. M.; Dounay, A. B.; Evrard, E.; Gan, X.; Ghosh, S.; Kim, J.-Y.; Parikh, V. D.; Tuttle, J. B.; Verhoest, P. R. A General Strategy for the Synthesis of Cyclic *N*-Aryl Hydroxamic Acids via Partial Nitro Group Reduction. *J. Org. Chem.* **2011**, *76*, 3484−3497.
(41) Methoxy substitution was not evaluated at the R^3 position due to chemical instability of this compound and analogous alkoxy analogues.
(42) Copeland, R. A. *Evaluation of Enzyme Inhibitors in Drug Discovery: A Guide for Medicinal Chemists and Pharmacologists*; Wiley: Hoboken, NJ, 2005; pp 1−265.
(43) KYNA concentrations can be maximally decreased by approximately 80% from basal values at a dose of 32 mg/kg, sc. The remaining 20% KYNA is likely biosynthesized by KAT I.